J Mater Sci: Mater Electron (2022) 33:20223–20228

Solar-blind ultraviolet photodetector based on Ti-doped Ga_2O_3/Si p–n heterojunction

Ugur Harmanci[1,*], M. Tahir Gulluoglu[1], Ferhat Aslan[2], Abdullah Atilgan[3,4], and Abdullah Yildiz[3]

[1] Department of Electric and Electronic Engineering, Faculty of Engineering, Harran University, 63190 Sanliurfa, Turkey
[2] Department of Physics, Faculty of Art and Science, Harran University, 63190 Sanliurfa, Turkey
[3] Department of Energy Systems Engineering, Faculty of Engineering and Natural Sciences, Ankara Yildirim Beyazıt University, 06010 Ankara, Turkey
[4] Central Research Laboratory Application and Research Center, Ankara Yildirim Beyazıt University, 06010 Ankara, Turkey

Received: 6 May 2022
Accepted: 25 July 2022
Published online: 12 August 2022

ABSTRACT

A solar-blind ultraviolet photodetector based on Ti-doped Ga_2O_3/Si *p–n* heterojunction is demonstrated for the first time. It is found that the heterojunction quality forming between Ga_2O_3 and Si becomes better after Ti incorporation in Ga_2O_3. The current–voltage and temporal response measurements show that the detector based on Ti-doped Ga_2O_3/Si *p–n* heterojunction has a responsivity of 0.382 A/W and a fast rise time of 73 ms as well, which are much better than those undoped Ga_2O_3/Si *p–n* heterojunction analogues.

1 Introduction

Solar-blind ultraviolet photodetectors (SBUPs) have been recognized as efficient devices with potential for various military and civil applications. In the past few years, diligent efforts have been chased in SBUPs for improvement of the performance using diverse functional materials such as $Al_xG_{1-x}N$, $Mg_xZn_{1-x}O$, and Ga_2O_3 (GO) [1]. Nevertheless, the main path of performance degradation in SBUPs based on $Al_xG_{1-x}N$ and $Mg_xZn_{1-x}O$ is the presence of a significant amount of density of defect states originated from alloying process [2, 3]. This averts the photoresponse properties of the photodetector because of an increase in the dark current. Owing to the unnecessity of alloying process and its superior features such as having an eligible wide bandgap and inexpensive cost, GO becomes a good candidate for probing a SBUP. Since undoped GO is an electrical insulator due to its wide bandgap, Mg, Zn, Sn, Si, and Sb elements were introduced as dopants to particularly improve its photoelectrical properties. When divalent (Mg^{2+} and Zn^{2+}) and tetravalent (Ti^{4+}, Si^{4+}, and Sn^{4+}) ions substitute the site of trivalent Ga^{3+} in the lattice of GO, p-type and n-type Ga_2O_3 are found, respectively [4–8]. Many researchers reported that doped GO also outperforms its undoped analogue in terms of photodetector performance [4–8]. Although

Address correspondence to E-mail: uharmanci@harran.edu.tr

https://doi.org/10.1007/s10854-022-08840-3

a SBUP based on Ti-doped Ga_2O_3 (TGO)/sapphire Schottky heterojunction was reported that it has already good photoelectrical properties [6], to the best of our knowledge, examination of a SBUP consisting of TGO/Si p–n heterojunction has not been reported yet. Herein, we report the design and preparation of TGO/Si p–n heterojunction obtained via spin-coating process for SBUP.

2 Experimental

Gallium nitrate hydrate ($Ga(NO_3)_3{\cdot}xH_2O$; ALDRICH, 99.9%), monoethanolamine [MEA;C_2H_7NO; EMSUR, 99.5%], and 2-methoxyethanol ($C_3H_8O_2$; ALDRICH, 99.8%), were used for the preparation of Ga_2O_3 solution as precursor material, stabilizer, and solvent material, respectively. $Ga(NO_3)_3{\cdot}xH_2O$ molarity was 0.2 molar, while $Ga(NO_3)3{\cdot}xH_2O$ and MEA;C_2H_7NO molarity were determined as one-to-one. To investigate the effect of titanium dopant, Ga_2O_3 solutions were prepared as undoped, Ti/Ga of 3 at% doped. The prepared solutions were mixed for 24 h at 60 °C to obtain a homogeneous and clear solution. Using a standard procedure, Si (100) were cleaned given elsewhere [9]. Then, the solutions were coated on the substrates at 2000 rpm for 30 s by spin-coating technique. The coated samples were dried at 150 °C for 10 min. Finally, the samples were annealed at 900 °C. Silver was applied as front and back contacts to the samples utilizing the screen-printing technique [10, 11]. The metal contacts were heated at 150 °C for 10 min. Then, the samples were characterized using standard techniques describe elsewhere [10, 11]. The *I–V* characteristics of the devices were recorded under UV-C (254 nm, 1.12 mW/cm^2) irradiation. Figure 1a shows the schematic structure of fabricated TGO/Si SBUP.

3 Results and discussion

To verify the formation of Ti-doped Ga_2O_3, EDS measurements was performed (Fig. 1b). One can obviously distinguish the peak position of Ti from others, which are Ga and O. The results clearly corroborate the presence of Ti ion used as doping source in the Ga_2O_3 structure. Ti/Ga atomic ratio is determined as 3% for TGO. It is important to highlight that no indication for unintended dopant can be deduced. The morphology of the films was studied by SEM. Uniform and homogeneous GO and TGO layers were deposited on the Si substrates with similar thicknesses of 450 nm, as it is revealed from SEM cross-sectional image (the inset of Fig. 1b).

The charge balance is maintained after inclusion of Ti ions in Ga_2O_3 lattice as it was reported for other material systems [12–16]. Note that ionic radius of Ga^{3+} (Ti^{4+}) is 0.047 nm (0.042 nm) and 0.062 nm (0.060 nm) for coordination number of 4 and 6, respectively. Since ionic sizes of Ga^{3+} and Ti^{4+} are close to each other, Ti ions occupy the host Ga_2O_3 lattice constituting solid solution. This occupation can be expressed by the reaction of $Ti \rightarrow Ti_{Ga} + V_{Ga}^{x}$. Here, Ti_{Ga} is Ti^{4+} ion substituted for Ga^{3+}, while V_{Ga}^{x} is the Ga^{3+}-ion vacancy of neutral charge [17].

The optical properties of the films deposited on quartz substrates are collected in Fig. 2. Typically, the films having similar smoothness and compactness with the same thickness exhibit similar transmittance

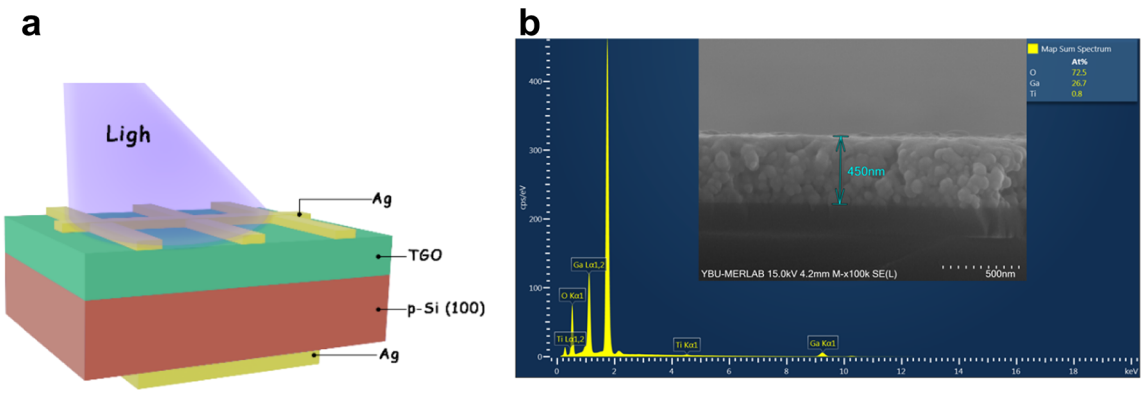

Fig. 1 **a** Schematic representation of the fabricated TGO/Si SBUP. **b** EDX for the TGO (Table: composition of O, Ga and Ti content extracted from EDS results). The inset of Fig. 1b depicts cross-sectional image SEM image of the TGO

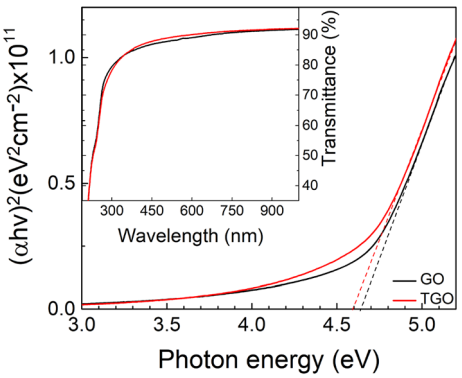

Fig. 2 Tauc's plots for the films. The inset of Fig. 3 shows the transmittance spectra of the films

spectrum. A slight decrease in transmittance implying a weak absorption around 300 nm can be ascribed to Ti-related defect level below the conduction band edge of Ga_2O_3 [6]. However, the TGO demonstrates slightly more transparency in visible region. Therefore, the presence of Ti-dopant will not obviously influence the harvesting of light through emitter layer. Decreased transmittance in deep ultraviolet region under 280 nm is here implied that the films can be employed as an emitter layer of SBUPs. Moreover, the more transparency of the Ti-doped Ga_2O_3 in the visible region might be associated with its decreasing refractive index depending on structural changes after dopant [18]. The results indicate that the light absorption edge had a slight red-shift for the TGO, which should be attributed to the decrease in the bandgap [17]. Using Tauc's equation, the bandgap energy of the films can be estimated [19].

$$(\alpha hv)^2 = C(hv - E_g) \quad (1)$$

where α is the absorption coefficient, hv is the incident photon energy and C is a constant. By extrapolating a straight line to the $(\alpha hv)^2 = 0$ axis in the plots of the $(\alpha hv)^2$ versus E_g, the value of E_g of GO and TGO were found to be 4.64 and 4.59 eV, respectively. These values are in agreement with those published elsewhere [6, 17].

Band diagram of Ti-doped Ga_2O_3/Si p–n heterojunction is given in Fig. 3. Some parameters were taken from elsewhere [20]. To investigate the optoelectronic performance of the GO/p-Si and TGO/p-Si devices, the current–voltage (I–V) characteristics in the dark and under light are shown in Fig. 4a. To comprehend SBUP behavior, the heterojunction occurring between Ga_2O_3 and p-Si can be qualitatively examined through realignment of band positions under reversed bias. In this case, majority carriers, i.e., electrons from Ga_2O_3-side to Si-side and holes from Si-side to Ga_2O_3-side cannot exceed high potential barrier, leading to a substantial reduction of current in dark. At this time, only minority carriers are responsible for the poor dark current. However, once the junction is illuminated by 254 nm light, the light is absorbed by the device and photogenerated electron–hole pairs occur at the depletion region of the junction. They are immediately separated under electric field forming in the depletion region. Ultimately, electrons transport from Si-side to Ga_2O_3-side, while holes transport from Ga_2O_3-side to Si-side, leading to an improvement in the photocurrent under reverse bias. As seen from Fig. 4a, the contribution of majority carriers to electric current is insignificant under forward bias for TGO/Si heterojunction, only minority carriers play a role in determining of photocurrent under reverse bias. On the other hand, this is invalid for GO/Si heterojunction where both majority and minority carriers co-participate to the photocurrent. Namely, the photocurrent increases simultaneously under reverse and forward bias region. Additionally, one might also expect the charge carriers captured by trap states can participate in the carrier transport once the energy of the light coming onto the junction is larger than the trap depth [21–24]. These results imply that junction quality becomes better after Ti incorporation in Ga_2O_3/Si heterojunctions.

One can see that the devices evidently manifest the rectification behavior and a response to the illumination. The asymmetry ratio [I(at 10 V)/I(at − 10 V)] in the dark is deduced to be as 12 and 4.94, and the dark current (I_D) is 22.4 and 86.9 mA at − 10 V for GO/p-Si and TGO/p-Si devices, respectively. The dark current values are higher than those reported elsewhere for Ga_2O_3-based devices [6]. This can be originated from the employed deposition method itself and the interface defects occurring between Ga_2O_3 and Si heterojunction. Incorporation of Ti doping can also introduce undesired defects which trap mobile electrons, resulting in an increase in dark current value over its undoped counterpart. Under the light exposure, the photocurrent (I_L) at − 10 V bias is enhanced by 1.68 and 2.31 times for GO/p-Si and TGO/p-Si devices, respectively. These outcomes beckon that the devices attest being SBUPs.

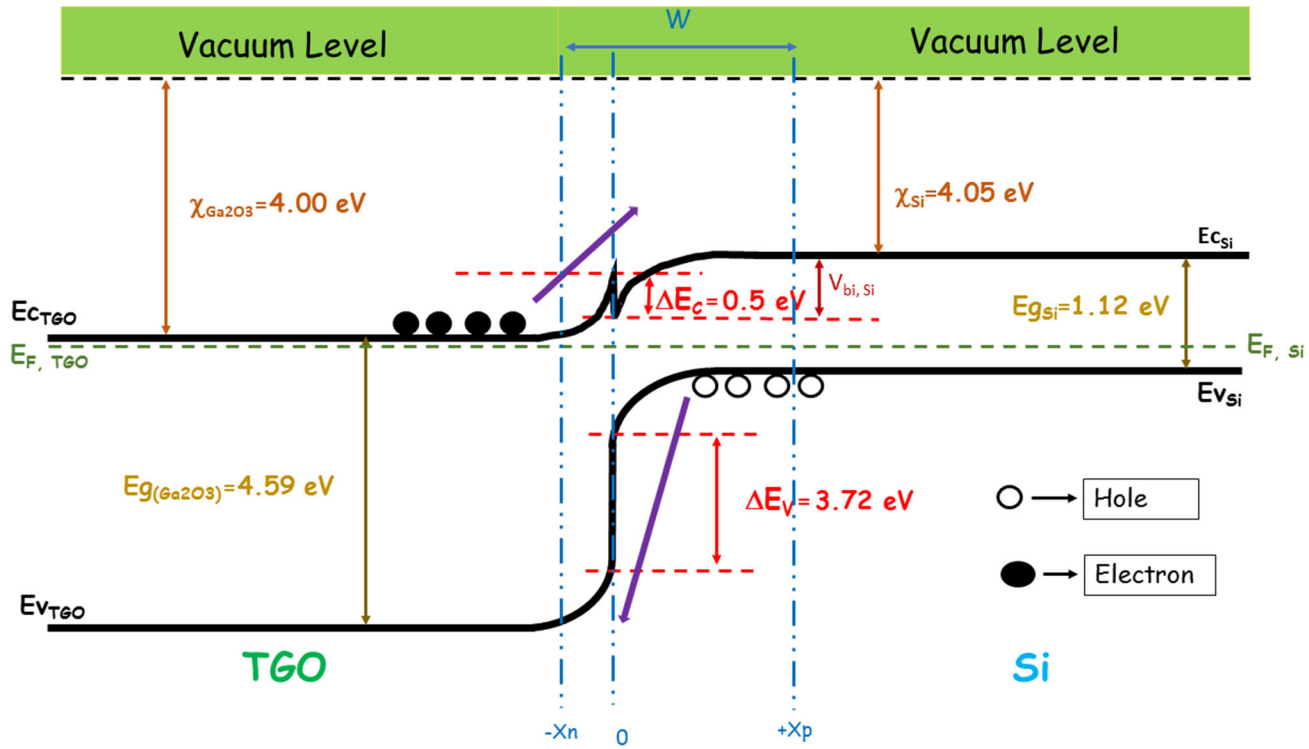

Fig. 3 Band diagram of Ti-doped Ga_2O_3/Si *p–n* heterojunction

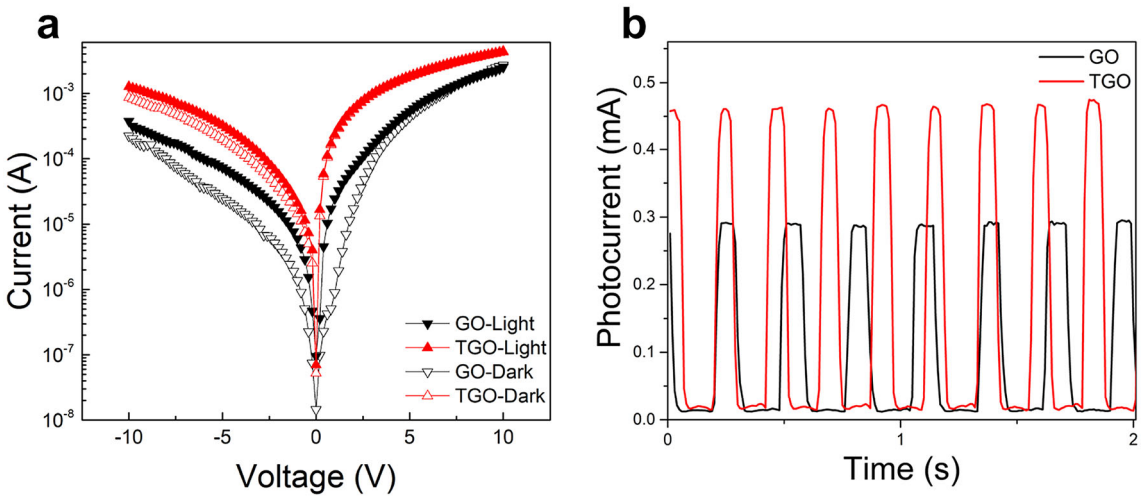

Fig. 4 **a** Semilogarithmic scale *I–V* curves of the photodetector measured in the dark and 254 nm UV illuminations. **b** Time-dependent photocurrent response under light illumination at − 10 V

The spectral responsivity (R) is considered as a critical parameter for evaluation of the performance of the device. It can be expressed as the photocurrent produced per optical power of the incident light. It can be obtained by the following equation [4–10]:

$$R = \frac{I_L - I_D}{P_{in}A} \quad (2)$$

where A is the effective area of the photodetector. With a bias voltage of − 10 V, a good photoresponsivity of 0.136 and 0.382 A/W was found under 254 nm for GO/p-Si and TGO/p-Si devices, respectively. The amelioration of photoresponsivity with dopant is in agreement with those reported previously [4–8]. It was also previously reported that light sensitivity of

Table 1 Comparison of the key parameters of SBUPs based on Ga_2O_3

Device	Responsivity (mA/W)	Bias (V)	τ_r (ms)	τ_d (ms)	References
Zn: Ga_2O_3/Sapphire	–	10	1950	250	[4]
Mg: Ga_2O_3/Al_2O_3	23.8	10	330	20	[5]
Si: Ga_2O_3/Quartz	1.44	25	880	180	[7]
Sn: Ga_2O_3/Al_2O_3	80	50	–	22	[8]
Ti: Ga_2O_3/p-Si	382	10	73	85	This work
Ga_2O_3/p-Si	–	20	4060	160	[29]

Ga_2O_3 increases with incorporation of Ti-dopant [17]. This might be attributed to an improvement electrical conductivity because of the occupation of Ti^{4+} ions to the location of Ga^{3+} ions and suppression of grain boundaries. The rejection ratio (R_{254nm}/R_{450nm}) is obtained to be 3.66 and 4.41 for GO/p-Si and TGO/p-Si devices, respectively, making it higher than the ratios of the previously reported Ga2O3 photodetectors. This result confirms that the Ti-dopant can contribute to improvement of the rejection ratio.

Furthermore, we conducted the calculation of other key photodetector parameters such as detectivity (D), external quantum efficiency (EQE), and linear dynamic range (LDR) [25–28]. The detectivity (D) is a measure of the device which reflects the ability of sensing the lowest detectable signal associated with the background noise, it can be given by

$$D = \sqrt{\frac{A}{2el_d}}R \tag{3}$$

where P_λ and A denote the light intensity and the illuminated area of the device, respectively. The D value is calculated to be 1.6×10^{10} and 2.3×10^{10} Jones for GO/p-Si and TGO/p-Si devices, respectively. This finding reveals better ability of TGO/p-Si device to succeed a high signal-to-noise ratio.

EQE is also a crucial parameter for expressing the aspect of photodetectors and it is described by

$$\mathrm{EQE} = \frac{I_{\mathrm{ph}}/}{P_{\mathrm{in}}/h\upsilon} = \frac{hc}{e\lambda}R \times 100\% \tag{4}$$

Here, c, h and λ denote the light velocity, Planck's constant, and the light wavelength, respectively. EQE is 46% and 130% for GO/p-Si and TGO/p-Si devices, respectively.

The performance of the devices can also be evaluated by linear dynamic range (LDR), LDR is expressed by

$$LDR = 20\log\left(\frac{I_{ph}}{I_d}\right) \tag{5}$$

The LDR value is estimated as 4.5 and 7.3 dB for GO/p-Si and TGO/p-Si devices, respectively.

All the mentioned parameters indicate a better skill of the device with Ti-dopant in photodetector performance, ascribable to an increased responsivity, accounting for the improved photocurrent. It is obvious that TGO/p-Si device is more excellent than GO/p-Si device."

Another figure of merit for SBUPs is the response time, which can be accurately evaluated from the transient photocurrent curve (Fig. 4b). The values of rise time (τ_r) and decay time (τ_d) given as the duration required for a 90% change of current were found to be 84 ms and 73 ms, and 132 ms and 85 ms at − 10V for GO/p-Si SBUP and TGO/p-Si SBUP, respectively. It is clear that both τ_r and τ_d values are superior for TGO/p-Si SBUP compared to GO/p-Si SBUP. Such a fast response time can be attributed to the rapid carrier separation and migration of the photogenerated carrier due to suppression of amount of defect states with Ti incorporation. Further, a comparison of the key parameters of various recently reported similar SBUPs is displayed in Table 1. Our device demonstrates much higher responsivity and a faster response time than that of doped Ga_2O_3-based SBUPs.

4 Conclusion

In summary, we experimentally demonstrated solar-blind ultraviolet photodetector performance of undoped Ga_2O_3/Si and Ti-doped Ga_2O_3/Si p–n heterojunctions obtained via spin-coating method. After Ti-dopant, the performance of the device was improved. The device of Ti-doped Ga_2O_3/Si exhibits better performance, including a high responsivity (0.382 A/W), high external quantum efficiency

(130%), high detectivity (2.3×10^{10} Jones) and quick response time (73 ms), being superior to most reported photodetectors based on undoped Ga_2O_3 and previously reported spin-coated Ga_2O_3 photodetectors. Finally, our approach provides a promising route for next-generation optoelectronic devices.

Acknowledgements

This work is based U.H's Ph.D thesis. It was supported by the Harran University BAP, Turkey under the Project Number 19084.

Author contributions

UH: Conceptualization, Methodology, Data curation, Writing—original draft. MTG: Supervision, Writing—review & editing, and Editing. FA: Investigation, Resources. AA: Visualization, Investigation. AY: Supervision, Writing—review & editing, and Editing. All authors read and approved the final manuscript.

Data availability

The datasets generated during and/or analyzed during the current study are available from the corresponding author on reasonable request.

Declarations

Conflict of interest The authors declare that they have no known competing interests.

References

1. U. Varshney et al., J. Mater. Chem. (2022). https://doi.org/10.1039/D1TC05101F
2. S.B. Lisesivdin et al., Semicond. Sci. Technol. **23**, 095008 (2008)
3. S.B. Lisesivdin et al., Opt. Adv. Mater. Rapid Comm. **1**, 467 (2007)
4. D. Guo et al., Electron. Mater. Lett. **13**, 483 (2017)
5. Y.P. Qian et al., Mater. Lett. **209**, 558 (2017)
6. W. Liu et al., Phys. Status Solidi RRL **15**, 2100411 (2021)
7. S.H. Jeong, T.K.O. Vu, E.K. Kim, J. Alloys Comp. **877**, 160291 (2021)
8. M.-M. Fan et al., Appl. Surf. Sci. **509**, 144867 (2020)
9. K. Ozel et al., J. Alloys Comp. **849**, 156628 (2020)
10. K. Ozel, A. Yildiz, Sens. Actuators A **315**, 112351 (2020)
11. M. Sbeta, A. Yildiz, Mater. Res. Exp. **6**, 085018 (2019)
12. Y. Gao et al., J. Am. Cer. Soc. **100**, 2901 (2017)
13. Y. Gao et al., ACS Appl. Electron. Mater. **1**, 961 (2019)
14. Y. Gao et al., Opt. Mater. **86**, 611 (2018)
15. Y. Gao et al., J. Lumin. **238**, 118235 (2021)
16. T. Serin et al., Phys. B Condens. Matter **406**, 3551 (2011)
17. A.A. Dankhel, Sol. State Sci. **20**, 54–58 (2013)
18. D. Mardare et al., Appl. Surf. Sci. **156**, 200 (2000)
19. T. Serin et al., Phys. Scr. **84**, 065703 (2011)
20. A. Verma et al., ACS Appl. Nano Mater. **5**, 4860 (2022)
21. R.K. Tripathi et al., J. Mater. Sci. Mater. Electron. **32**, 2535 (2021)
22. A. Yildiz, S.B. Lisesivdin, M. Kasap, D. Mardare, Optoelectron. Adv. Mater. Rapid Commun. **1**, 531–533 (2007)
23. D. Mardare et al., J. Appl. Phys. **112**, 073502 (2012)
24. A. Yildiz, H. Cansizoglu, T. Karabacak, Appl. Surf. Sci. **352**, 2 (2015)
25. A. Verma et al., Sens. Actuators A **321**, 112600 (2021)
26. C. Gautam et al., Opt. Mater. **123**, 111860 (2022)
27. K. Ozel, A. Yildiz, Phys. Status Solidi RRL Rapid Res. Lett. **15**, 2100085 (2021)
28. K. Ozel, A. Yildiz, Semicond. Sci. Technol. **36**, 095001 (2021)
29. G. Shin et al., J. Chem. Eng. **35**, 574 (2018)